

Identification of Portimine B, a New Cell Permeable Spiroimine That Induces Apoptosis in Oral Squamous Cell Carcinoma

Andrew M. Fribley,^{*,†} Yue Xi,[†] Christina Makris,[§] Catharina Alves-de-Souza,[‡] Robert York,[‡] Carmelo Tomas,[‡] Jeffrey L. C. Wright,^{§,||} and Wendy K. Strangman^{*,||}

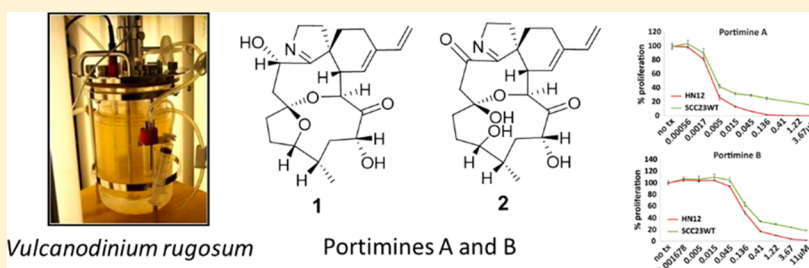
[†]Carman and Ann Adams Department of Pediatrics, Division of Hematology/Oncology and the Molecular Therapeutics Program, Karmanos Cancer Institute, Wayne State University, 421 East Canfield, Detroit, Michigan 48201, United States

[‡]Algal Resources Collection, MARBIONC at Crest Research Park, University of North Carolina Wilmington, 5600 Marvin Moss K. Lane, Wilmington, North Carolina 28409, United States

[§]Department of Chemistry and Biochemistry, University of North Carolina Wilmington, 601 South College Road, Wilmington, North Carolina 28403, United States

^{||}Biomolecular Discovery Group, MARBIONC at Crest Research Park, University of North Carolina Wilmington, 5600 Marvin Moss K. Lane, Wilmington, North Carolina 28409, United States

S Supporting Information



ABSTRACT: Spiroimines are a class of compounds produced by marine dinoflagellates with a wide range of toxicity and therapeutic potential. The smallest of the cyclic imines, portimine, is far less toxic than other known members in several animal models. Portimine has also been shown to induce apoptosis and reduce the growth of a variety of cancer cell lines at low nanomolar concentrations. In an effort to discover new spiroimines, the current study undertook a metabolomic analysis of cultures of cyclic imine-producing dinoflagellates, and a new analog of portimine was discovered in which the five-membered cyclic ether is open. Further scrutiny with human oral cavity squamous cell carcinoma (OCSCC) cell lines revealed that the open ring congener was less potent than portimine A but could still lead to the accumulation of apoptotic gene transcripts, fragment genomic DNA, and reduce cancer cell proliferation in the range of 100–200 nM.

KEYWORDS: Portimine, spiroimine, *Vulcanodinium rugosum*, dinoflagellate, apoptosis, OCSCC, natural products

Spiroimine toxins are a growing family of compounds produced by members of several genera of harmful algal bloom-forming marine dinoflagellates. They include compound families described as gymnodimines,¹ spiroalides,² pinnatoxins,³ prorocentrolides,⁴ pteriatoxins,⁵ spiro-prorocentrimines,⁶ and the recently described portimine.⁷ Like many dinoflagellate compounds, spiroimine toxins are macrocycles containing cyclic ether rings and a characteristic five- to seven-membered cyclic imine with a spiro-linkage to a six-membered cyclohexene pharmacophore. Portimine is the only identified member with a five-membered cyclic imine or an eight-membered cyclic ether ring.⁷

The spiroimine family of toxins have gained notoriety as a potential threat to human health through ingestion of contaminated seafood. While no episodes of human intoxication have been linked to cyclic-imine contaminated foodstuffs, animal studies have shown that some of these “fast-acting” toxins can be fatal when injected or ingested even

at low quantities ($\mu\text{g}/\text{kg}$).^{2,8,9} A mechanism of action for the toxicity of these compounds has been put forth whereby they might lead to respiratory paralysis through the inhibition of muscular and neuronal nicotinic acetylcholine receptors.¹⁰ As has been observed with other natural products, subtoxic concentrations of several cyclic imines have demonstrated efficacy in preclinical pathophysiologic rodent models and human cell lines. Gymnodinime A and 13-desmethylspiroalide were able to cross the blood-brain barrier and improve protein expression profiles and behavioral tasks in murine Alzheimer’s disease models.^{11,12} The smallest member of the cyclic imine family, portimine, displays the least in vivo toxicity in animal models with an IP LD_{50} of 1570 $\mu\text{g}/\text{kg}$ and no effects observed

Received: October 9, 2018

Accepted: December 26, 2018

Published: December 26, 2018

at 500–700 $\mu\text{g}/\text{kg}$ compared to other spiroimines such as desmethyl spiroside C ($\text{LD}_{50} = 7 \mu\text{g}/\text{kg}$), pinnatoxin F ($\text{LD}_{50} = 16 \mu\text{g}/\text{kg}$), and gymnodimine ($\text{LD}_{50} = 96 \mu\text{g}/\text{kg}$).⁷ The cytotoxicity of portimine was apparent in cancer cells and was nearly 100 times more potent than pinnatoxin ($\sim 3 \text{ nM}$ vs $1 \mu\text{M}$ for pinnatoxin F).⁷ A recent report provided important mechanistic insight into the antiproliferative nature of these compounds with a series of experiments that identified the ability of portimine to induce BCL2-dependent apoptosis in Jurkat acute T cell leukemia cells.¹³

A comparative semitargeted metabolomics investigation, with known spiroimine producers housed in the UNC Wilmington Marine Biotechnology (MARBIONC) Algal Resources Collection (ARC), was performed to assess the breadth of spiroimine production across dinoflagellates and to identify new congeners. These examinations focused on three strains of disparate spiroimine producing genera, *Karenia selliformis*, a producer of gymnodimines;¹⁴ *Alexandrium ostenfeldii*, a producer of both gymnodimines and spiroolides;¹⁵ and *Vulcanodinium rugosum*, the producer of portimine.⁷ Principal component analysis (PCA) of the three species and a corresponding dendrogram visualization of the metabolomics data highlighted a distinct subset of metabolites unique to a strain of *V. rugosum* isolated from a 2004 ballast water collection in Port Tampa Bay Florida (Figure 1A,B).¹⁶ This strain has been shown to produce portimine but not the structurally related pinnatoxins coproduced by other *V.*

rugosum strains.¹⁷ Further interrogation of the *V. rugosum* metabolite profile through S-plot analysis of the cell-specific compounds vs the media components indicated that portimine is one of the major secondary metabolites produced (Figure 1C). An additional mass feature was identified from this analysis that eluted closely with portimine, and the HRMS data suggested a related compound. Based on these data, the *V. rugosum* culture was scaled up in $4 \times 10\text{L}$ photobioreactors for purification, structural characterization, and cytotoxicity profiling in oral cavity squamous cell carcinoma (OSCC) cells.

Portimine B **2** (Figure 2) was isolated as a white powder. The molecular formula was established by HRESIMS as

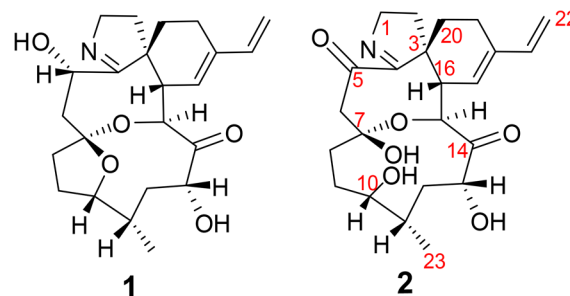


Figure 2. Structures of portimine A (**1**) and portimine B (**2**).

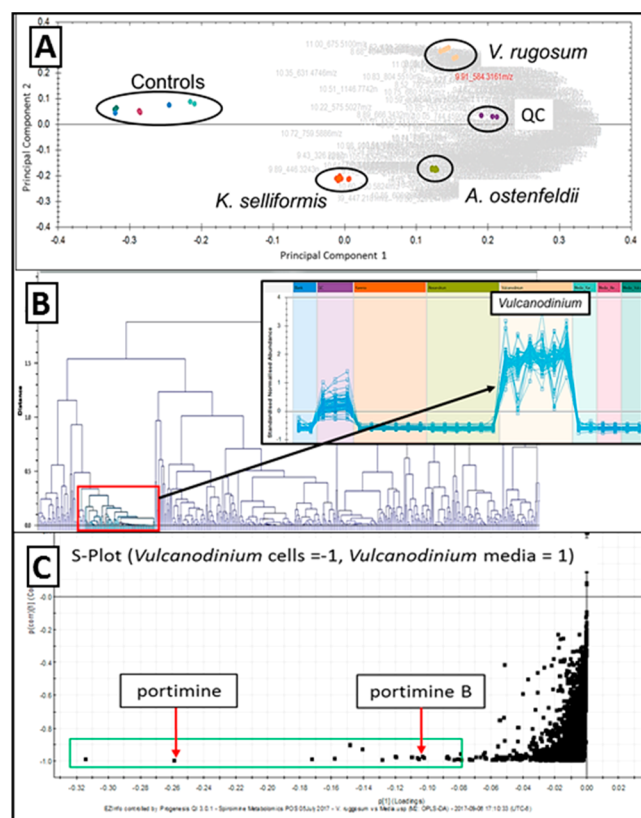


Figure 1. (A) PCA plot of MARBIONC ARC cyclic imine producers. (B) Dendrogram analysis metabolites from the ARC cultures with expansion of abundance profiles for *V. rugosum* specific mass features. (C) S-Plot expansion of *V. rugosum* cell-specific mass features (mass-retention pairing represented by black dots) with portimines A and B highlighted.

$\text{C}_{23}\text{H}_{31}\text{NO}_6$ (m/z 418.2230 $[\text{M} + \text{H}]^+$; calcd for $\text{C}_{23}\text{H}_{32}\text{NO}_6$ 418.2230, $\Delta = 0.0$ ppm), requiring nine degrees of unsaturation. This is 16 amu greater than portimine, indicating the addition of an oxygen ($\text{C}_{23}\text{H}_{31}\text{NO}_5$) while retaining the same degrees of unsaturation.

Detailed analysis of 1D and 2D NMR spectra, and comparison with published data, revealed that much of the structure of **2** was similar to **1**, including the spiroimine ring system and the conjugated exomethylene (S1).⁷ Several apparent differences were critical in assigning the planar structure of this new compound. Specifically, the hydroxymethine at position 5 ($\delta\text{H}/\delta\text{C}$ 4.50, 65.6) observed in **1** was no longer present in **2**. Instead, a carbonyl (δC 201.4) appearing in the HMBC NMR spectrum of **2** was assigned to this position (S1). This substitution was further corroborated by changes in the chemical shift and the splitting pattern of the adjacent methylene at position 6 (S1).

Based on the molecular formula, an additional oxygen remained to be accounted for while maintaining the calculated degrees of unsaturation. Examination of the 1D and 2D NMR data indicated that one of the spiroketal rings was now open and that an additional hydroxyl was present. Key in determining which of the two possible rings had opened was an HMBC correlation from the hydroxymethine ($\delta\text{H}/\delta\text{C}$ 4.63, 72.4) at position 15 to the hemiketal carbon at position 7 (δC 107.2), which would only be possible if the eight-membered ring was still intact. Thus, it became evident that the five-membered ether ring was no longer present in **2** and that hydroxyls were located on carbons 7 and 10 (Figure 2B).

Comparison with NOESY data (from **2**) with assignments for portimine indicated that all of the correlations for portimine were present in **2**, suggesting they shared a similar 3D structure (Table S1). The stereoisomeric configurations at carbons 7 and 10 were modeled in Chem3D relative to the assumed configuration of carbon 16, and under the constraints

of the observed NOESY correlations, to confirm these assignments.⁷

The fact that **1** and other cyclic imine toxins are bioavailable has been established in preclinical vertebrate-derived cell models that include amphibian,^{18,19} murine,²⁰ and human cancer.^{13,21} The ability of any compound to passively permeate lipid membranes is an important measure of potential bioavailability and toxicity, a concept that becomes increasingly important when a substance is studied in a preclinical setting. Parallel artificial membrane permeability assays (PAMPA) were employed to more thoroughly explore the pharmacokinetic properties of **1** and **2**. A 1 mg/mL solution of a semipurified crude extract of *V. rugosum* was incubated in the donor compartment of a 96-well PAMPA plate for 6 h. The relative concentrations of **1** and **2** were quantitated by UPLC-HRMS qTOF-MS for the donor and acceptor wells via the extracted ion chromatograms (supplemental) and compared to verapamil (highly permeable) and prednisone (low permeability) controls (tested at 100 μ M). Compounds **1** and **2** displayed passive permeability similar to verapamil, with **2** slightly lower than **1** (Table 1). These data suggest that the

Table 1. PAMPA Assays with the Percentage of the Indicated Compound Identified with UPLC-HRMS qTOF-MS in the Acceptor Well after 6 h

compound	permeability
verapamil	54 (\pm 2)
prednisone	12 (\pm 3)
portimine A (1)	54 (\pm 4)
portimine B (2)	35 (\pm 5)

portimine scaffold, in terms of permeability, has a promising pharmacokinetic profile and support the continued investigation of **1** and **2** in preclinical models of human diseases.

Oral cavity squamous cell carcinoma (OSCC) is an underfunded and understudied major cancer²² that annually claims approximately 10,000 lives in the USA. Despite a trending increase in purely synthetic and biological drugs, 1/3 of all cancer drugs approved by the FDA between 1981 and 2014 were natural products or natural product derivatives.²³ Work from our laboratory has demonstrated that OSCC cell lines are sensitive to a variety of natural products isolated from aquatic microbes.^{24,25} The OSCC cell lines UMSCC23 and HN12 were cultured with increasing concentrations of purified (98% by UPLC-PDA) **1** and **2**. ATP-based luminescent proliferation assays revealed dose-dependent inhibition over a 36 h period, with **1** demonstrating substantially reduced IC₅₀ values compared to **2** (Figure 3A). A previous report that **1** could induce apoptosis in human leukemic T cell lymphoblasts¹³ prompted the evaluation of apoptotic transcripts in cDNA libraries generated from **1**- and **2**-treated OSCC cultures. The experimentally determined IC₅₀ for each compound was applied over a 36 h period. RT-qPCR analysis revealed an accumulation of pro-apoptotic *GADD45 α* , *NOXA*, and *DR5* and antiapoptotic *BCL2* (Figure 3B). In general, increases in gene expression were observed at earlier time points for **1**. During homeostasis, *BCL2* holds proapoptotic proteins (i.e., *BAX* and *BAK*) in an inactive state. The initiation of intrinsic (mitochondrial-mediated) apoptosis is preceded by increased levels of *NOXA* and other BH3-only *BCL2* family members which then titrate *BCL2* away from *BAX* and *BAK*. The release of *BCL2* allows cytochrome *c* to

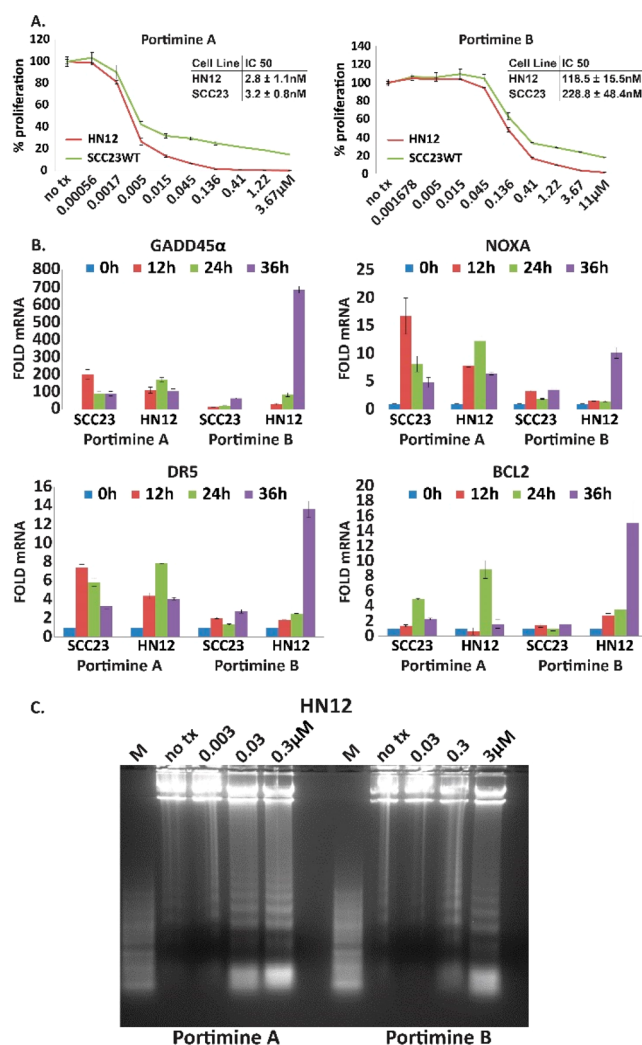


Figure 3. Portimines induce apoptosis and reduce OSCC proliferation. (A) ATP-based proliferation assays after 48 h exposure to **1** (left) and **2** (right); error bars indicate SD. (B) Taqman RT-qPCR analysis of cDNA libraries generated from OSCC cell lines treated with the IC₅₀ (determined in A) for each compound; error bars represent SEM from three identical experiments performed in triplicate. (C) Electrophoretic resolution of genomic DNA harvested from HN12 cells exposed to **1** (left) or **2** (right) for 48 h.

rove from the space between the inner and outer mitochondrial membranes to the cytosol, leading to apoptosome formation and the sequential cleavage (activation) of caspases 9 and 3. The ability of **1** and **2** to activate both apoptotic and antiapoptotic genes indicates that parallel antithetical responses are commenced whereby apoptosis is initiated by *NOXA*, and an attempt to survive the challenge is provided by *BCL2*. Consistent with this notion, *BCL2* overexpression could almost entirely ameliorate the apoptotic effects of **1**.¹³ Finally, DNA laddering has been used previously to demonstrate the ability of natural products to induce apoptosis in oral cancer cells.^{25–27} The IC₅₀ for **1** and **2** as well as a semilog dose (above and below) were used to treat HN12 cells for 48 h. Electrophoretically resolved genomic DNA demonstrated dose-dependent laddering, a hallmark of apoptosis (Figure 3C). These data indicate that **1** and **2** induced apoptosis and reduced the proliferation of oral cancer cells.

The current study has identified a previously unreported spiroimine isolated from *V. rugosum* collected off the coast of Florida, USA. The compound is structurally related to portimine and is designated herein as portimine B. A notable feature of this new congener is the opening of one of the spiroketal rings and the addition of a hydroxyl group at the same location. We hypothesize that increased polarity and decreased rigidity resulting from this feature were contributing factors to the observation that **2** was observed to be less potent than **1** with respect to the activation of apoptosis and the reduced proliferation in OCSCC cultures. Selwood et al. reported that the LD₅₀ for mice injected with intraperitoneal portimine was 1570 µg/kg and noted this to be much lower than other imine shellfish toxins.⁷ When considered in the light of the current study, and the anticancer activity of **1** noted in leukemia cell cultures,¹³ further preclinical studies with *in vivo* cancer models and drug combinations are warranted to more fully appreciate what the translational value of this very potent class of polycyclic ethers might be.

■ ASSOCIATED CONTENT

📄 Supporting Information

The Supporting Information is available free of charge on the ACS Publications website at DOI: 10.1021/acsmchemlett.8b00473.

Experimental design, NMR spectra, and mass spectra (PDF)

■ AUTHOR INFORMATION

Corresponding Authors

*E-mail: strangmanw@uncw.edu

*E-mail: afribley@med.wayne.edu

ORCID

Jeffrey L. C. Wright: 0000-0001-9299-9744

Wendy K. Strangman: 0000-0002-6911-4909

Author Contributions

The manuscript was written through contributions of all authors. All authors have given approval to the final version of the manuscript.

Funding

This work was supported by The Children's Hospital of Michigan Foundation (to A.M.F.) and the Departments of Pediatrics and Otolaryngology at the Wayne State University School of Medicine (to A.M.F.) and the Marbionic Program at UNC Wilmington (to C.A., C.M., R.Y., C.T., J.L.C.W., W.K.S.).

Notes

The authors declare no competing financial interest.

■ ABBREVIATIONS

OCSCC, oral cavity squamous cell carcinoma; RT-qPCR, real time quantitative polymerase chain reaction; ER stress, endoplasmic reticulum stress; UPR, unfolded protein response

■ REFERENCES

- (1) Seki, T.; Satake, M.; Mackenzie, L.; Kaspar, H. F.; Yasumoto, T. Gymnodimine, a new marine toxin of unprecedented structure isolated from New Zealand oysters and the dinoflagellate, *Gymnodinium* sp. *Tetrahedron Lett.* **1995**, *36* (39), 7093–7096.
- (2) Hu, T.; Curtis, J. M.; Oshima, Y.; Quilliam, M. A.; Walter, J. A.; Watson-Wright, W. M.; Wright, J. L. Spirolides B and D, two novel

macrocycles isolated from the digestive glands of shellfish. *J. Chem. Soc., Chem. Commun.* **1995**, No. 20, 2159–2161.

- (3) Uemura, D.; Chou, T.; Haino, T.; Nagatsu, A.; Fukuzawa, S.; Zheng, S.-z.; Chen, H.-s. Pinnatoxin A: a toxic amphoteric macrocycle from the Okinawan bivalve *Pinna muricata*. *J. Am. Chem. Soc.* **1995**, *117* (3), 1155–1156.

- (4) Torigoe, K.; Murata, M.; Yasumoto, T.; Iwashita, T. Prorocentrolide, a toxic nitrogenous macrocycle from a marine dinoflagellate, *Prorocentrum lima*. *J. Am. Chem. Soc.* **1988**, *110* (23), 7876–7877.

- (5) Takada, N.; Umemura, N.; Suenaga, K.; Uemura, D. Structural determination of pteriatoxins A, B and C, extremely potent toxins from the bivalve *Pteria penguin*. *Tetrahedron Lett.* **2001**, *42* (20), 3495–3497.

- (6) Lu, C.-K.; Lee, G.-H.; Huang, R.; Chou, H.-N. Spiroprorocentrimine, a novel macrocyclic lactone from a benthic *Prorocentrum* sp. of Taiwan. *Tetrahedron Lett.* **2001**, *42* (9), 1713–1716.

- (7) Selwood, A. I.; Wilkins, A. L.; Munday, R.; Shi, F.; Rhodes, L. L.; Holland, P. T. Portimine: a bioactive metabolite from the benthic dinoflagellate *Vulcanodinium rugosum*. *Tetrahedron Lett.* **2013**, *54* (35), 4705–4707.

- (8) Munday, R.; Towers, N. R.; Mackenzie, L.; Beuzenberg, V.; Holland, P. T.; Miles, C. O. Acute toxicity of gymnodimine to mice. *Toxicol.* **2004**, *44* (2), 173–178.

- (9) Munday, R.; Selwood, A. I.; Rhodes, L. Acute toxicity of pinnatoxins E, F and G to mice. *Toxicol.* **2012**, *60* (6), 995–999.

- (10) Kharrat, R.; Servent, D.; Girard, E.; Ouanounou, G.; Amar, M.; Marrouchi, R.; Benoit, E.; Molgó, J. The marine phycotoxin gymnodimine targets muscular and neuronal nicotinic acetylcholine receptor subtypes with high affinity. *J. Neurochem.* **2008**, *107* (4), 952–963.

- (11) Alonso, E.; Vale, C.; Vieytes, M. R.; Laferla, F. M.; Giménez-Llort, L.; Botana, L. M. 13-Desmethyl spiroside-C is neuroprotective and reduces intracellular A β and hyperphosphorylated tau in vitro. *Neurochem. Int.* **2011**, *59* (7), 1056–1065.

- (12) Alonso, E.; Otero, P.; Vale, C.; Alfonso, A.; Antelo, A.; Gimenez-Llort, L.; Chabaud, L.; Guillou, C.; Botana, L. M. Benefit of 13-desmethyl spiroside C treatment in triple transgenic mouse model of Alzheimer disease: beta-amyloid and neuronal markers improvement. *Curr. Alzheimer Res.* **2013**, *10* (3), 279–289.

- (13) Cuddihy, S. L.; Drake, S.; Harwood, D. T.; Selwood, A. I.; McNabb, P. S.; Hampton, M. B. The marine cytotoxin portimine is a potent and selective inducer of apoptosis. *Apoptosis* **2016**, *21* (12), 1447–1452.

- (14) Miles, C. O.; Wilkins, A. L.; Stirling, D. J.; MacKenzie, A. L. Gymnodimine C, an isomer of gymnodimine B, from *Karenia selliformis*. *J. Agric. Food Chem.* **2003**, *51* (16), 4838–4840.

- (15) Van Wagoner, R. M.; Misner, I.; Tomas, C. R.; Wright, J. L. Occurrence of 12-methylgymnodimine in a spiroside-producing dinoflagellate *Alexandrium peruvianum* and the biogenetic implications. *Tetrahedron Lett.* **2011**, *52* (33), 4243–4246.

- (16) Garrett, M. J.; Puchlutegui, C.; Selwood, A. I.; Wolny, J. L. Identification of the harmful dinoflagellate *Vulcanodinium rugosum* recovered from a ballast tank of a globally traveled ship in Port Tampa Bay, Florida, USA. *Harmful Algae* **2014**, *39*, 202–209.

- (17) Rhodes, L.; Smith, K.; Selwood, A.; McNabb, P.; Munday, R.; Suda, S.; Molenaar, S.; Hallegraef, G. Dinoflagellate *Vulcanodinium rugosum* identified as the causative organism of pinnatoxins in Australia, New Zealand and Japan. *Phycologia* **2011**, *50* (6), 624–628.

- (18) Kharrat, R.; Servent, D.; Girard, E.; Ouanounou, G.; Amar, M.; Marrouchi, R.; Benoit, E.; Molgó, J. The marine phycotoxin gymnodimine targets muscular and neuronal nicotinic acetylcholine receptor subtypes with high affinity. *J. Neurochem.* **2008**, *107* (4), 952–63.

- (19) Araoz, R.; Ouanounou, G.; Iorga, B. I.; Goudet, A.; Alili, D.; Amar, M.; Benoit, E.; Molgó, J.; Servent, D. The neurotoxic effect of 13,19-didesmethyl and 13-desmethyl spiroside C phycotoxins is

mainly mediated by nicotinic rather than muscarinic acetylcholine receptors. *Toxicol. Sci.* **2015**, *147* (1), 156–67.

(20) Hauser, T. A.; Hepler, C. D.; Kombo, D. C.; Grinevich, V. P.; Kiser, M. N.; Hooker, D. N.; Zhang, J.; Mountfort, D.; Selwood, A.; Akireddy, S. R.; Letchworth, S. R.; Yohannes, D. Comparison of acetylcholine receptor interactions of the marine toxins, 13-desmethylspirolide C and gymnodimine. *Neuropharmacology* **2012**, *62* (7), 2239–50.

(21) Wandscheer, C. B.; Vilarino, N.; Espina, B.; Louzao, M. C.; Botana, L. M. Human muscarinic acetylcholine receptors are a target of the marine toxin 13-desmethyl C spirolide. *Chem. Res. Toxicol.* **2010**, *23* (11), 1753–61.

(22) Fribley, A. M.; Svider, P. F.; Warner, B. M.; Garshott, D. M.; Raza, S. N.; Kirkwood, K. L. Recent Trends in Oral Cavity Cancer Research Support in the United States. *J. Dent. Res.* **2017**, *96* (1), 17–22.

(23) Newman, D. J.; Cragg, G. M. Natural Products as Sources of New Drugs from 1981 to 2014. *J. Nat. Prod.* **2016**, *79* (3), 629–61.

(24) Cruz, P. G.; Fribley, A. M.; Miller, J. R.; Larsen, M. J.; Schultz, P. J.; Jacob, R. T.; Tamayo-Castillo, G.; Kaufman, R. J.; Sherman, D. H. Novel Lobophorins Inhibit Oral Cancer Cell Growth and Induce Atf4- and Chop-Dependent Cell Death in Murine Fibroblasts. *ACS Med. Chem. Lett.* **2015**, *6* (8), 877–81.

(25) Sidhu, A.; Miller, J. R.; Tripathi, A.; Garshott, D. M.; Brownell, A. L.; Chiego, D. J.; Arevang, C.; Zeng, Q.; Jackson, L. C.; Bechler, S. A.; Callaghan, M. U.; Yoo, G. H.; Sethi, S.; Lin, H. S.; Callaghan, J. H.; Tamayo-Castillo, G.; Sherman, D. H.; Kaufman, R. J.; Fribley, A. M. Borrelidin Induces the Unfolded Protein Response in Oral Cancer Cells and Chop-Dependent Apoptosis. *ACS Med. Chem. Lett.* **2015**, *6* (11), 1122–7.

(26) Xi, Y.; Garshott, D. M.; Brownell, A. L.; Yoo, G. H.; Lin, H. S.; Freeburg, T. L.; Yoo, N. G.; Kaufman, R. J.; Callaghan, M. U.; Fribley, A. M. Cantharidins induce ER stress and a terminal unfolded protein response in OSCC. *J. Dent. Res.* **2015**, *94* (2), 320–9.

(27) Fribley, A. M.; Miller, J. R.; Brownell, A. L.; Garshott, D. M.; Zeng, Q.; Reist, T. E.; Narula, N.; Cai, P.; Xi, Y.; Callaghan, M. U.; Kodali, V.; Kaufman, R. J. Celastrol induces unfolded protein response-dependent cell death in head and neck cancer. *Exp. Cell Res.* **2015**, *330* (2), 412–22.